ELECTRONIC SUPPLEMENTARY INFORMATION

Removal of CO_2 from CH_4 and CO_2 capture in the presence of H_2O vapour in NOTT-401

Hugo A. Lara-García, Maximiliano R. Gonzalez, Juan H. González-Estefan, Pedro Sánchez-Camacho, Enrique Lima and Ilich A. Ibarra*

Instituto de Investigaciones en Materiales, Universidad Nacional Autónoma de México, Circuito Exterior s/n, CU, Del. Coyoacán, 04510, México D. F., Mexico.
E-mail: argel@unam.mx

1. Scheme of the binuclear [$M_2(\mu_2$-OH)] building block

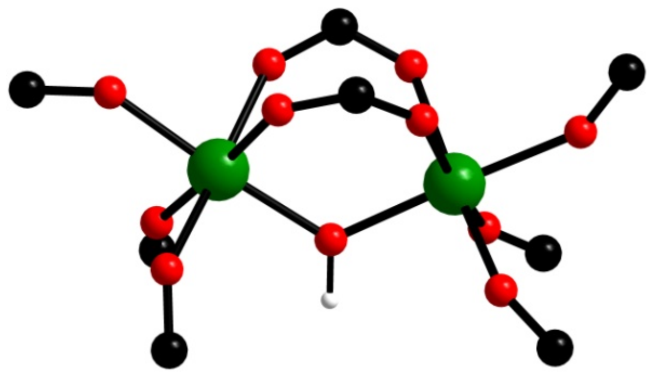

Scheme S1: Binuclear building block of two metal ions oxygen octahedra bridged by a μ_2-hydroxo group. Green, red, black and white spheres represent M (metal ion such as In(III) or Sc(III)), O, C and H atoms, respectively.

2. Materials and Measurements

All reagents and solvents were used as received from commercial suppliers without further purification. Powder X-ray diffraction (PXRD) data were collected under ambient conditions on a Bruker AXD D8 Advance diffractometer operated at 160 W (40 kV, 40 mA) for Cu $K\alpha_1$ (λ= 1.5406 Å). Thermal gravimetric analysis (TGA) was performed under N_2 at a scan rate of 2 °C/min using a TA Instruments Q500HR analyser. N_2 adsorption was carried out in a conventional volumetric technique by a Micromeritics ASAP 2020 sorptometer. The surface area was calculated using the BET method based on adsorption data in the partial pressure (p/p_0) range 0.01 to 0.04. Dynamic and isothermal experiments were performed using a humidity-controlled thermobalance (TA Instruments, model Q5000SA) at 30 ^{o}C and a relative humidity (RH) of 40%. A catalytic reactor system (BEL-REA, BEL Japan) coupled to a Bruker TENSER 27 FTIR was employed to measure the gas selectivity.

3. TGA plots

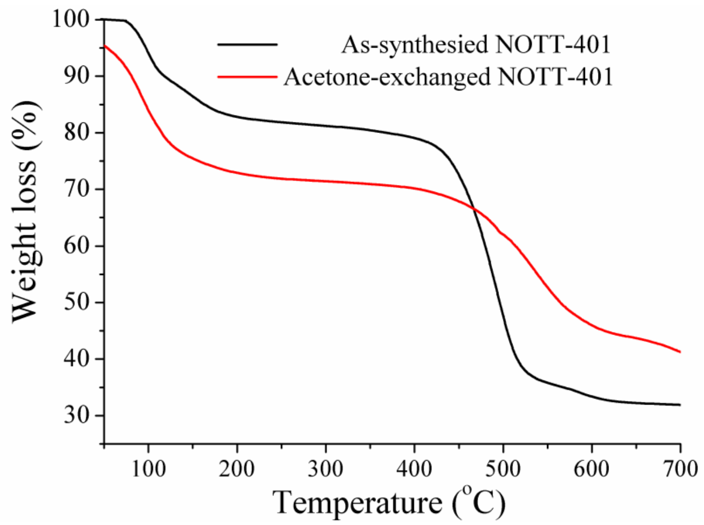

Fig. S1: TGA analyses of as-synthesised NOTT-401 (black line) and acetone-exchanged NOTT-401 (red line).

4. Powder X-ray Diffraction Patterns

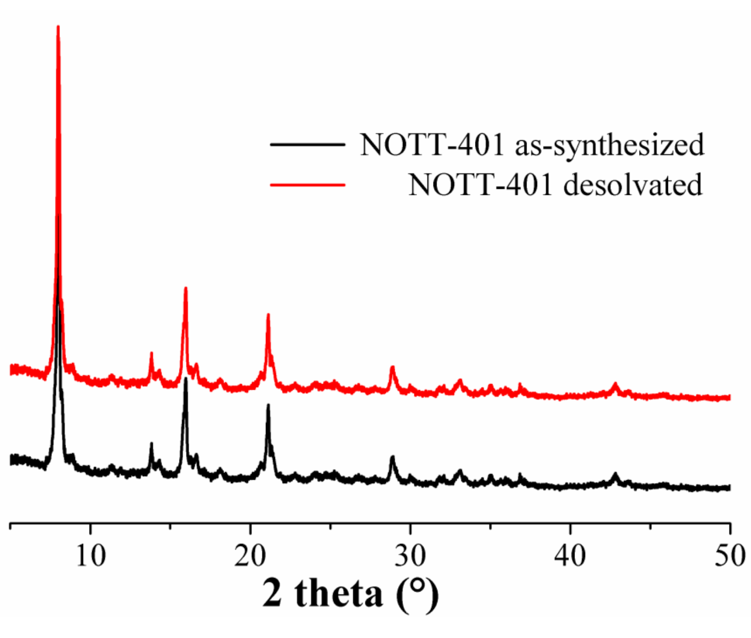

Fig. S2: PXRD patters of as-synthesised (black) and desolvated (red) NOTT-401.

5. Catalytic Reactor System (BEL-REA) for the Gas CO_2 and CH_4 Selectivity Experiments

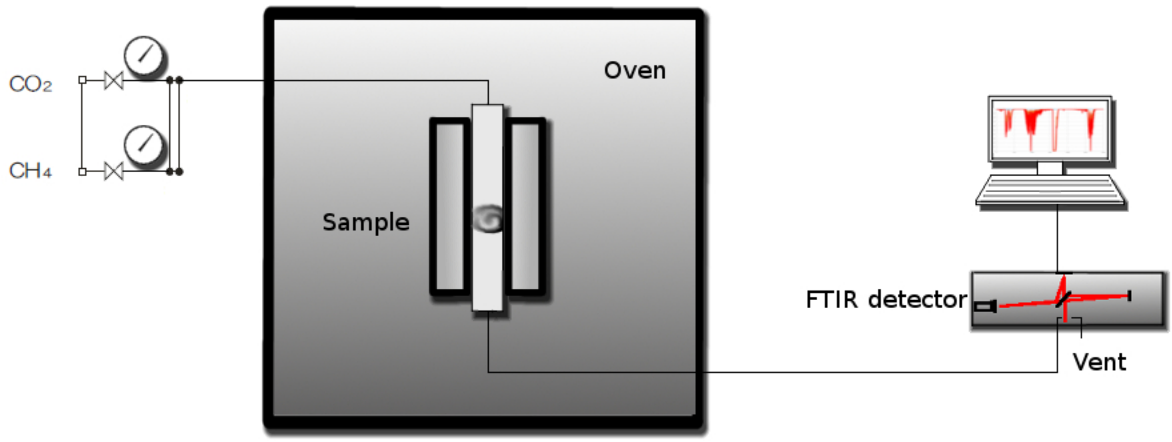

Fig. S3: Catalytic reactor system (BEL-REA) system.

6. FTIR Spectra

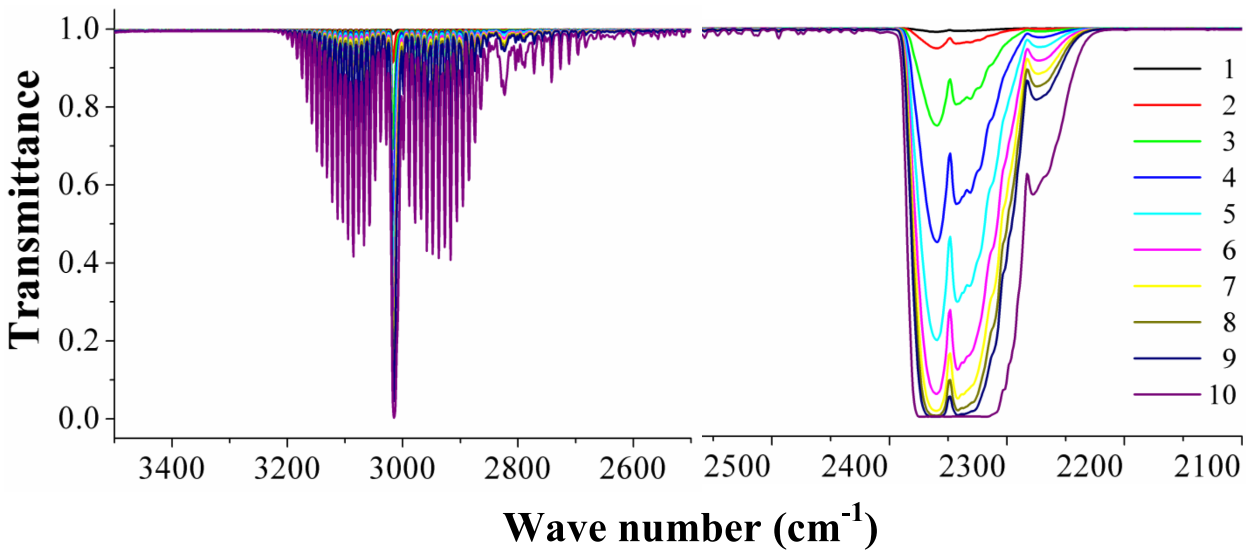

Fig S4: FTIR spectra of the resulting binary equimolar (0.13 mmol min^{-1}) gas-mixture flow (that passed through the activated NOTT-401 sample).

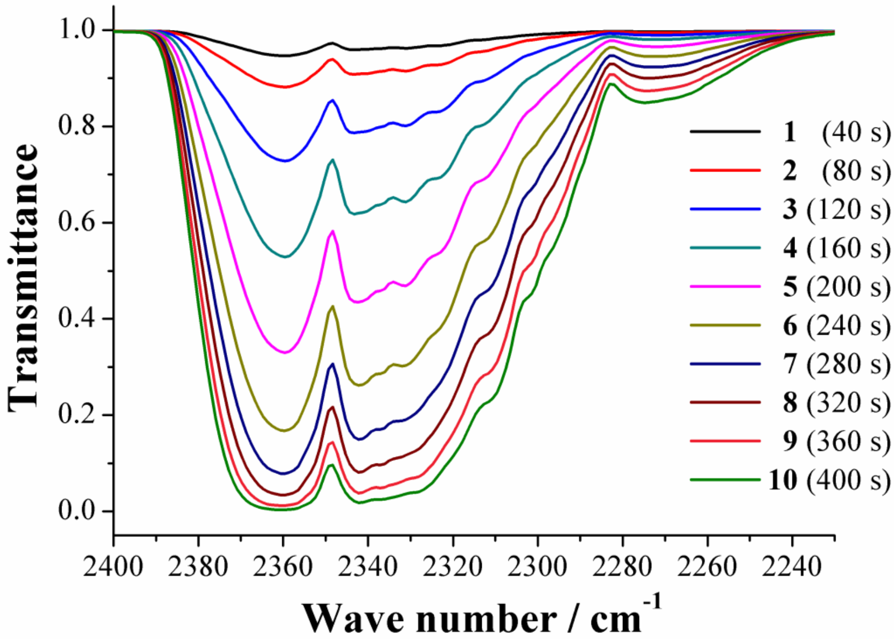

Fig S5: FTIR spectra of the resulting flow of only CO_2 gas (0.13 mmol min^{-1}) that passed through the activated NOTT-401 sample.

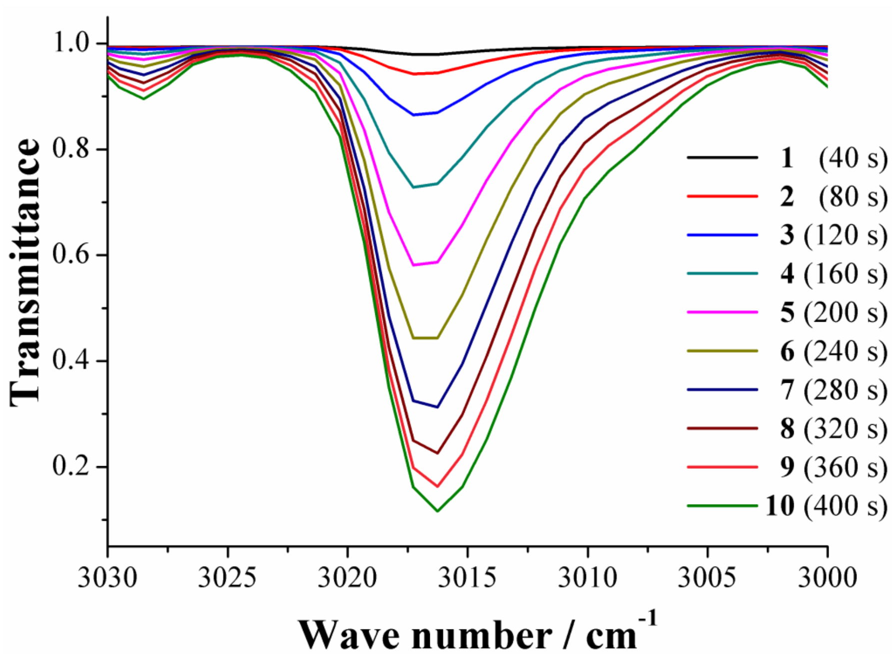

Fig S6: FTIR spectra of the resulting flow of only CH_4 gas (0.13 mmol min^{-1}) that passed through the activated NOTT-401 sample.

7. Polynomial Regressions

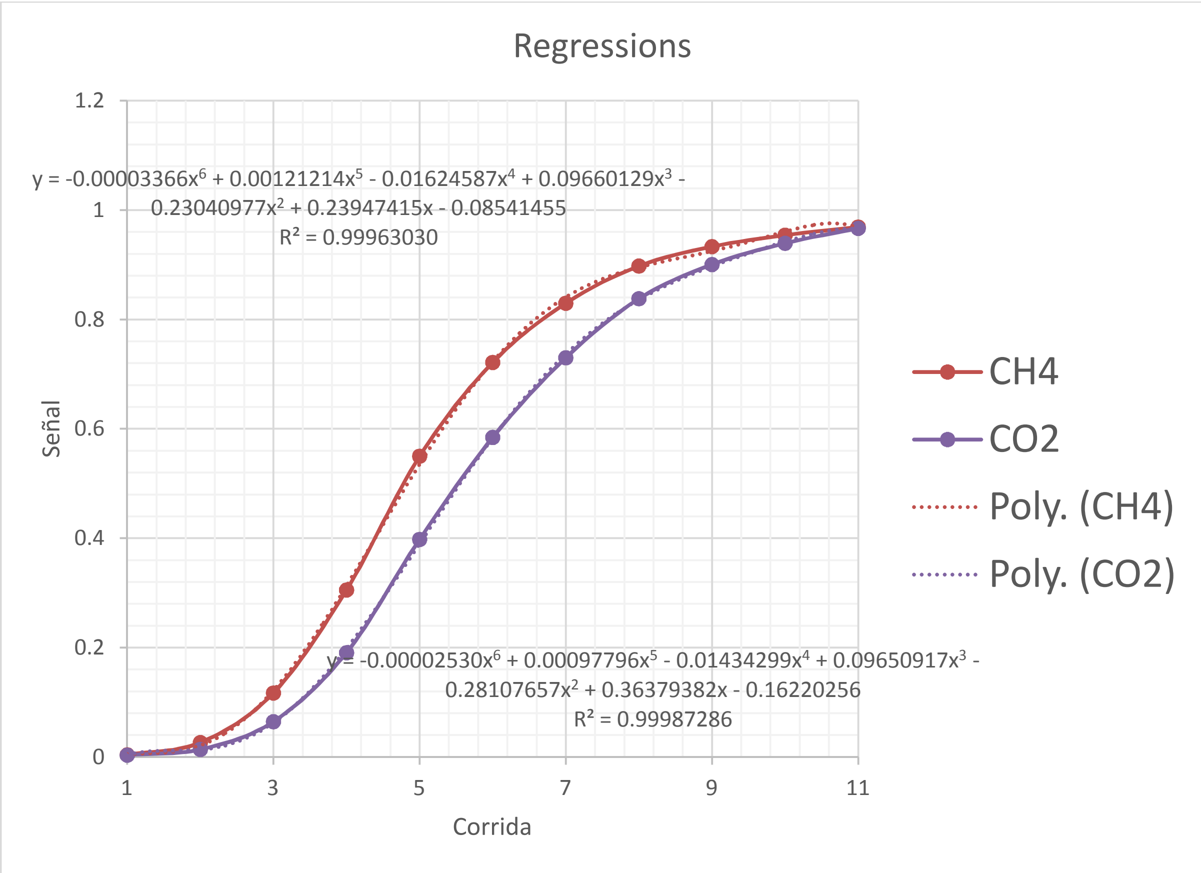

Fig S7: Polynomial regressions of the normalised intensities on Fig. 2 left.

By taking the derivative of both functions:
$f(x) = -0.00003366x^6 + 0.00121214x^5 - 0.01624587x^4 + 0.09660129x^3 - 0.23040977x^2 + 0.23947415x - 0.08541455$
$g(x) = -0.00002530x^6 + 0.00097796x^5 - 0.01434299x^4 + 0.09650917x^3 - 0.28107657x^2 + 0.36379382x - 0.16220256$
it is possible to plot both derivative functions ($df(x)/dx$ and $dg(x)/dx$) and find the maximum of both derivates. The difference of these derivates is equal to 0.59 scan which corresponds to ~ 23.53 s.

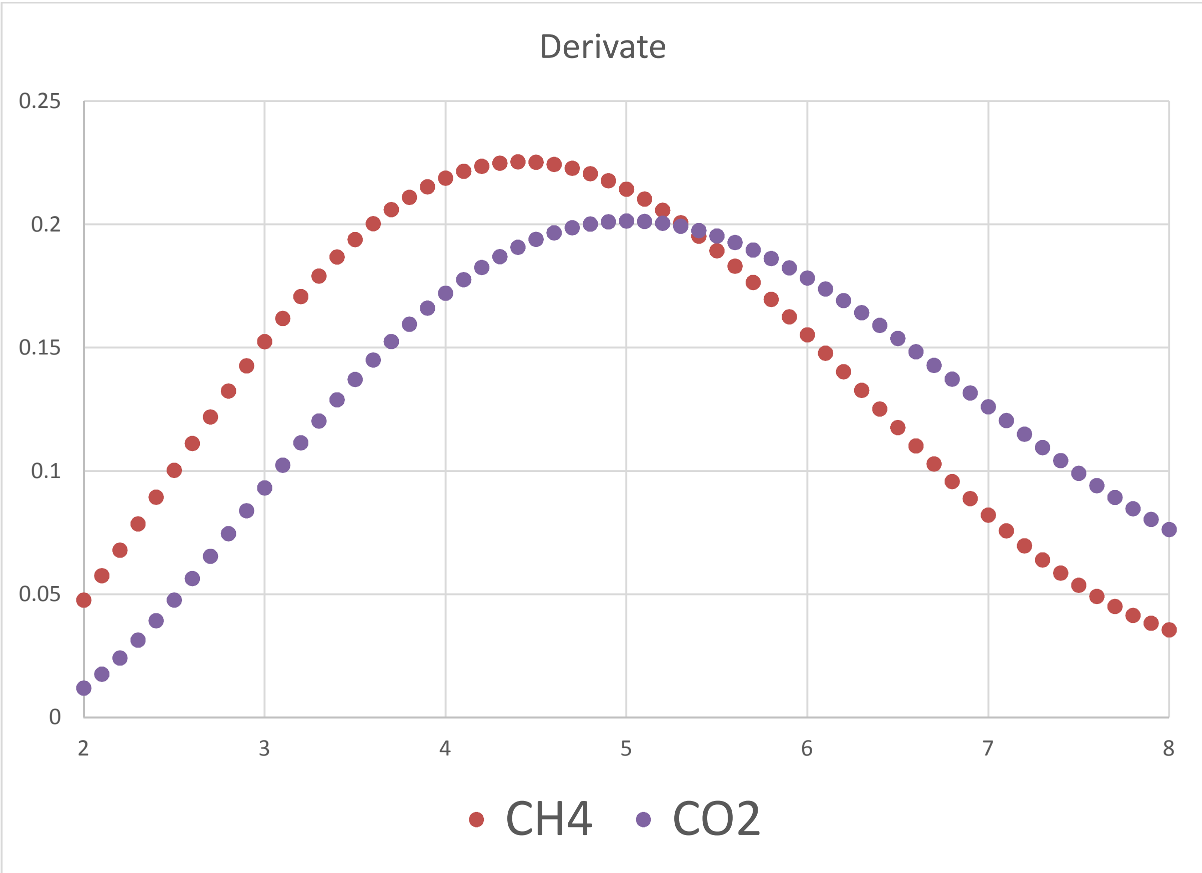

Fig. S8: Derivate functions (df(x)/dx and dg(x)/dx) coming from polynomial regressions of the normalised intensities on Fig. 2 left. Methane in red and carbon dioxide in blue.

8. Normalised characteristic FTIR intensities of CO_2 and CH_4 as a function of the number of scans

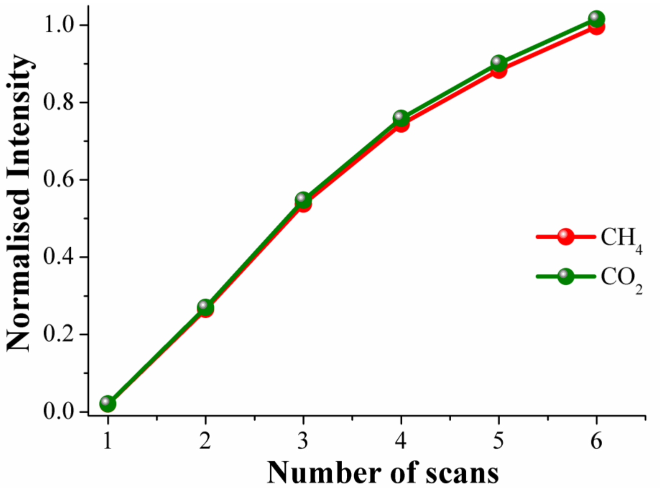

Fig. S9: Normalised characteristic FTIR intensities of CO_2 and CH_4 as a function of the number of scans from a resulting exit exhaust of the binary equimolar (0.13 mmol min^{-1}) gas-mixture of CO_2 and CH_4 in PCM-14.

9. PXRD and Kinetic Isotherms

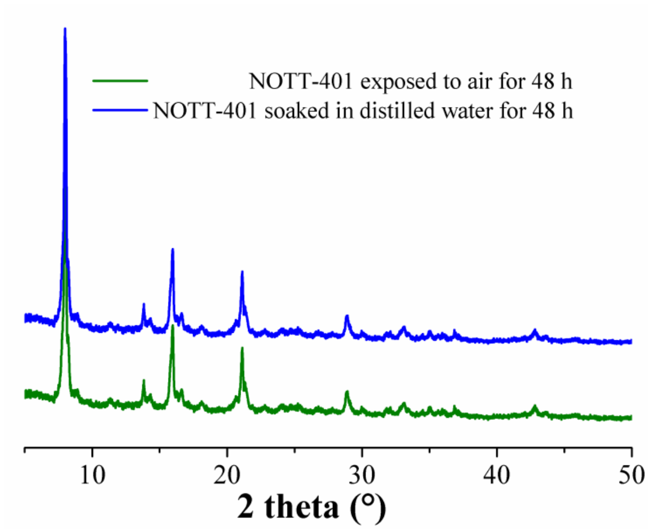

Fig. S10: Powder X-ray diffractions patterns of NOTT-401 after being exposed to air (green) and soaked in distilled water (blue) for 48 h.

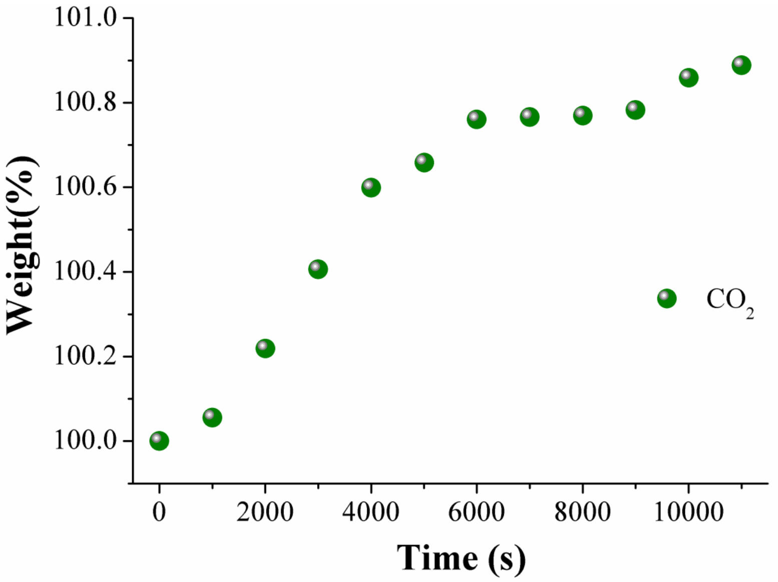

Fig. S11: Kinetic isotherms carried out at 30 ^{o}C and 40% RH with a CO_2 flow of 60 mL/min in PCM-14.